УДК 551.465.7

© *С. Д. Мартьянов*[1], *А. Ю. Дворников*[1], *В. А. Рябченко*[1], *Д. В. Сеин*[1,2], *С. М. Гордеева*[1,3]
[1]Институт океанологии им. П. П. Ширшова РАН, г. Москва
[2]Институт Альфреда Вегенера, Центр Полярных и Морских исследований им. Гельмгольца, г. Бремерхафен, Германия
[3]Российский государственный гидрометеорологический университет, г. Санкт-Петербург
martyanov.sd@gmail.com

ИЗУЧЕНИЕ СВЯЗИ ПЕРВИЧНОЙ ПРОДУКЦИИ И МОРСКОГО ЛЬДА В АРКТИЧЕСКИХ МОРЯХ: ОЦЕНКИ НА ОСНОВЕ МАЛОКОМПОНЕНТНОЙ МОДЕЛИ МОРСКОЙ ЭКОСИСТЕМЫ

Статья поступила в редакцию 09.04.2018, после доработки 23.04.2018.

Работа направлена на дальнейшую разработку региональной совместной эко-термогидродинамической модели арктических морей с целью использования ее для лучшего понимания процессов взаимодействия динамических и экосистемных процессов в океане при изменяющемся климате в Арктике. В качестве термогидродинамического блока используется MITgcm, в качестве экосистемного — оригинальная 7-компонентная модель океанской биогеохимии пелагиали, включающей в себя углеродный цикл. Приводятся результаты модельного климатического расчета на 40-летний период для региона арктического шельфа (Карское, Баренцево и Белое моря). Полученные оценки пространственного распределения концентрации хлорофилла-а в поверхностном слое позволили яснее понять влияние морского льда на первичную продукцию в арктическом регионе, в том числе в условиях меняющегося климата, который приводит к заметному сокращению площади ледяного покрова в Северном Ледовитом океане. Получена связь между площадью маргинальной зоны льда и первичной продукцией: время наступления их весенне-летнего пика полностью совпадает при высоком коэффициенте корреляции (0.87), доказывая важность данной зоны в функционировании морской экосистемы. Межгодовая изменчивость средних за гидрологический год (с октября по сентябрь) интегральной первичной продукции и суммарной площади льда, как и ожидалось, демонстрирует противофазность, что позволяет утверждать, что малая ледовитость в предшествующую зиму является основной причиной увеличения первичной продукции в текущем году.

Ключевые слова: изменение климата, моделирование морских экосистем, первичная продукция, морской лед, Баренцево море, Карское море.

S. D. Martyanov[1], *A. Yu. Dvornikov*[1], *V. A. Ryabchenko*[1], *D. V. Sein*[1,2], *S. M. Gordeeva*[1,3]
[1]Shirshov Institute of Oceanology, Russian Academy of Sciences; Moscow, Russia
[2]Alfred Wegener Institute, Helmholtz Centre for Polar and Marine Research; Bremerhaven, Germany
[3]Russian State Hydrometeorological University; St. Petersburg, Russia

INVESTIGATION OF THE RELATIONSHIP BETWEEN PRIMARY PRODUCTION AND SEA ICE IN THE ARCTIC SEAS: ASSESSMENTS BASED ON A SMALL-COMPONENT MODEL OF MARINE ECOSYSTEM

Received 09.04.2018, in final form 23.04.2018.

The work is focused on the further development of a regional coupled eco-thermohydrodynamic model of the Arctic seas with the aim of using it to better understand the interaction of dynamic and ecosystem processes in the ocean under a changing climate in the Arctic. We used the MITgcm as a thermohydrodynamic block and an original 7-component ecosystem model which includes the carbon cycle as an ocean biogeochemistry block. The results of a model climatic run for a 40-year modern period for the Arctic shelf region (Kara, Barents and White Seas) are presented. The estimates of the spatial distribution of the chlorophyll-a concentration in the surface layer have clarified the effect of sea ice on primary

Ссылка для цитирования: *Мартьянов С. Д., Дворников А. Ю., Рябченко В. А., Сеин Д. В., Гордеева С. М.* Изучение связи первичной продукции и морского льда в арктических морях: оценки на основе малокомпонентной модели морской экосистемы // Фундаментальная и прикладная гидрофизика. 2018. Т. 11, № 2. С. 108—117.

For citation: *Martyanov S. D., Dvornikov A. Yu., Ryabchenko V. A., Sein D. V., Gordeeva S. M.* Investigation of the relationship between primary production and sea ice in the arctic seas: assessments based on a small-component model of marine ecosystem. *Fundamentalnaya i Prikladnaya Gidrofizika.* 2018, 11, 2, 108—117.

doi: 10.7868/S2073667318020107

production in the Arctic seas, including under conditions of a changing climate that leads to a significant reduction of ice cover in the Arctic Ocean. The clear relationship between the area of the marginal ice zone and primary production has been obtained: the moments of their spring-summer peaks coincide completely and they are highly correlated (0.87), proving the importance of this zone in the functioning of the marine ecosystem. As expected, the interannual variability of the integrated primary production and the total sea ice area (both averaged over the hydrological year — from October to September) have demonstrated an antiphase oscillation which means that the reduced sea ice cover area in the previous winter is one of the main reasons for the increase in primary production in the current year.

Key words: climate change, marine ecosystem modeling, primary production, sea ice, Barents Sea, Kara Sea.

1. Introduction. In recent decades the sharp reduction of the ice cover in the Arctic Ocean has led to the extending area of water open for free penetration of photosynthetically active radiation (PAR) into the water column. During the period 1998—2006 the average annual primary production in this area of the World Ocean increased by 30 % [1]. Despite the increasing use of satellite measurement tools in the study of the functioning of marine ecosystems and their large contribution in our knowledge, remote sensing alone is still not enough. At present, only the usage of numerical mathematical models of marine biogeochemical cycles, properly calibrated and verified against observational data, allows estimating the fraction of primary production that occurs under the ice or below the surface layer.

According to the Research Fronts — reports revealing the most hot and top-cited research directions in various fields of knowledge [2—4], climate change due to carbon dioxide exchange between the ocean and the atmosphere in the last glaciation, effects of ocean acidification on marine ecosystems, application of regional climate models for the prediction of surface temperature and precipitation and studies on the model optimization, the impact of the reduction of ice cover in the Arctic on climate, the role of atmospheric carbon in the climate system, and evaluation of the contribution of terrestrial carbon cycle in climate models were recognized as ones of the most relevant and promising directions of scientific research in the field of earth sciences. Therefore, many relevant and urgent tasks in the field of earth sciences today include the development of detailed regional models, including ocean and sea models, which allow studying and assessing the contribution of climate change to the changes in hydrological and biogeochemical processes.

Implementation of detailed coupled thermohydrodynamic and ecosystem models is associated with certain difficulties. First, if the task is to describe the biogeochemical processes on a small scale in detail then the problem of determining the key parameters of the marine ecosystem may arise. Such data are scarce or absent at all, therefore in practice some generalized parameters obtained for other regions or during the calibration of any other models (e.g. [5]) are often used. Secondly, the practical use of detailed coupled three-dimensional models faces the problem of the lack of sufficient computing resources. As a result, a compromise between the detailed description of processes and the necessary model simplification has to be found.

Today there exist several models adapted to reproduce biogeochemical cycles in the Arctic Ocean or its marginal seas. For example, a coupled model of circulation and biogeochemistry with coarse resolution was used in [6] to study the carbon dioxide fluxes in the Arctic Ocean, with the MEDUSA (Model of Ecosystem Dynamics, nutrient Utilization, Sequestration and Acidification) [7, 8] model being used as a biogeochemical module. MEDUSA implements the phytoplankton separation into different size-groups and describes the cycles of nitrogen, silicon and iron. In works [9, 10] this coupled modeling system was used to study the functioning of the marine ecosystem and its various elements in the Arctic and showed good results consistent with observational data. An example of another model, used in [11] to assess the effect of ice cover reduction in the Arctic Ocean on primary production, is a joint model of circulation – sea ice – marine ecosystem of the Arctic Ocean, the biogeochemical component of which is the NEMURO model [12]. Calculations were carried out for the period 1988—2007 and showed a significant effect of decreasing the area of the ice cover on the marine planktonic ecosystem. In [13], the influence of Arctic ice cover reduction on the marine ecosystem was also studied, and an NPZD-pelagic model with several types of phytoplankton and nutrients based on [14, 15] was used. It is worth to mention the model of the Kara Sea ecosystem developed at the Shirshov Institute of Oceanology [16]. Also the study [17] considered the process of the local erosion of thermocline in the Barents Sea due to the passage of a cyclone over the sea which may cause an increase in productivity in this region

due to the upwelling of deep waters rich in nutrients. A fairly detailed description of some models of marine ecosystems currently available for the White Sea is given in the book [18]. We also would like to mention the recently developed model for the White Sea — Green JASMINE [19], the ecosystem block being the Italian model BFM [20, 21].

The present study, carried out within the framework of the EXOSYSTEM international project ("The impact of EXtreme events of future climates on the marine ecOSYSTEM in the Baltic and Barents Sea" of the ERA.Net RUS Plus Program), is focused on the further development of the regional coupled eco-thermohydrodynamic model of the Arctic seas with the aim to better understand the interaction of dynamic and ecosystem processes in the ocean under the changing climate in the Arctic. It presents the results of the model climatic calculation for a 40-year period (1966—2005) for the Arctic shelf region (Kara, Barents and White Seas) with external forcing (atmospheric forcing, conditions at open sea boundaries) obtained from the calculations of the modern climate (1920—2005) performed with the regional ocean model ROM in accordance with the scenario AR5 IPCC [22].

2. Methods

2.1. Coupled model. Calculation of the current climate for the Barents, Kara and White Seas was carried out using the Massachusetts Institute of Technology general circulation model (MITgcm) [23]. MITgcm is a general three-dimensional model of ocean circulation based on the primitive equations of hydrodynamics of an incompressible fluid in the Boussinesq approximation. The numerical algorithm is based on the finite volume method which ensures the exact conservation of mass and also accelerates the integration time of the model in comparison with models of similar spatial resolution based on finite element method [24]. The MITgcm sea ice model is based on the viscous-plastic dynamic-thermodynamic sea ice model described in [25—27] and modified in [28]. Despite the ability of the MITgcm to perform calculations for the non-hydrostatic formulation, only the hydrostatic mode of the model was used in the present study. This was dictated by a still relatively coarse horizontal resolution (in comparison with the vertical one). In addition, solving a complete non-hydrostatic problem for climatic model runs would require a much longer computational time.

The thermohydrodynamic model (MITgcm) was coupled with the three-dimensional 7-component model of the ocean pelagic biogeochemistry including the carbon cycle developed and tested earlier for the Barents Sea [29]. This biogeochemical model is a classical NPZD-based model of the lower trophic level of oceanic pelagic ecosystem (nitrates, phytoplankton, zooplankton, detritus) supplemented by a block of three state variables (total inorganic carbon, inorganic detritus — calcite, and alkalinity) describing the cycle of carbon in the ocean.

The described coupled eco-thermohydrodynamic model was adapted for the part of the Arctic Ocean including the White Sea, the Barents Sea and the Kara Sea. The computational grid is curvilinear quasi-orthogonal mesh with the North Pole transferred to the western hemisphere to achieve a more uniform spatial discretization. The grid consists of 544×518 cells in the horizontal plane and has 51 z-levels in the vertical direction (Fig. 1, see an insert). The model grid was constructed in such a way that the horizontal discretization throughout the model domain was approximately the same and equal to two nautical miles. This technique should increase the reliability of the obtained results due to the absence of computational errors associated with the heterogeneity of the computational grid in horizontal plane. In vertical direction the discreteness in the upper layers is 2—5 m, in the lower layers — up to 50 m. The time step for the main climatic runs was set equal to 120 seconds, the period of computations was 40 years (1966—2005).

Initial conditions, conditions at the open borders and atmospheric forcing were specified from the results of the model ROM [22]. This procedure ensured the consistency of these fields among each other. The river runoff was specified based on the climatic data. The inflow of organic and inorganic substances with river runoff was not taken into account due to the absence of data.

Calculations carried out on the Mistral computing cluster (Germany) have shown that the coupling of MITgcm and seven-component ecosystem model has not led to significant increase of the model integration time due to the parallel architecture of MITgcm and the significant computational resources of Mistral.

2.2. Model validation. Comparison of the observed and calculated sea ice thickness in February (averaged over the period 1990—2005) has shown that MITgcm, in general, correctly reproduces the spatial distribution and seasonal changes of sea ice in the model area (Fig. 2, see an insert). At the same time, as compared with the PIOMAS archive [30, 31], the model underestimates the ice thickness near the shores of islands, i.e. in the areas

where there is fast ice. For the model basin as a whole, the average annual computed thickness and area of the sea ice for the period 1990—2005 were less than those from the PIOMAS archive by 3.9 % and 1 %, respectively.

Calibration and validation of the ecosystem model used for the Barents Sea region was carried out earlier on the basis of a comparison with satellite data [29] and showed a good agreement between the calculated chlorophyll-*a* surface concentration and remote sensing data. In the current paper an additional calibration and validation of the same ecosystem model has been performed based on a comparison of the calculated chlorophyll-*a* concentration (Chla) and phytoplankton primary production (PP) with field measurements at several points whose position is shown in Fig. 1. These data were taken from the open database on primary production in the Arctic for the period 1954—2006 [32].

Fig. 3 shows the vertical profiles of calculated chlorophyll-*a* concentration and primary production which start at the depth of 2.5 m since the scalar fields are calculated at the center of the model cells and the thickness of the upper layer in the model is 5 m. Using the classic Redfield ratio (C:N:P = 106:16:1), the modeled concentrations of phytoplankton expressed in [mmol N/m^3] were recalculated into the concentration of phytoplankton organic carbon [mmol C/m^3] and then — into the chlorophyll-*a* concentration [mg/m^3], the constant chlorophyll-to-carbon ratio in phytoplankton being equal to 0.02.

As can be seen from Fig. 3, the model values of chlorophyll-*a* concentration and primary production are in a good agreement with the observational data at the sea surface in the vicinity of Svalbard. At the same time, the modeled subsurface maximum of the chlorophyll-*a* concentration is 14 m below the observed one. As for the remaining observation locations, the agreement between the modeled and observed vertical profiles is worse, but it would not be true to say that the model strongly distorts reality, given the complex nature of the simulated phenomenon in which not only physical but also biochemical processes play an important role. The orders of magnitude of the compared quantities in most cases are the same, and that is very important in the analysis of the integrated primary production (see below).

As a quantitative assessment of the agreement between the model results and observations the non-dimensional cost function was used. The cost function is a useful tool to compare data from two different sources and is recommended as a standard method for model validation [33]. The cost function is calculated as:

$$C = \left| \frac{M - D}{S} \right|,$$

where M — the mean value of the model results, D — the mean value of the in situ data, S — the standard deviation of the in situ data. According to paper [33], the following criteria of the goodness of fit between the model and observations were adopted: $0 < C \leq 1$ — very good, $1 < C \leq 2$ — good, $2 < C \leq 3$ — reasonable, $C > 3$ — poor. Based on the modeled and observation data, the values of the cost function have been calculated for five locations used for the model verification (table).

Despite the fact that the quality assessment based on the cost function is rather rough, it still can be used to evaluate the integral characteristics. As follows from the presented table, the model results adequately estimate the corresponding state of the measured values.

We emphasize a certain limitations of the model validation based on field measurements, which are associated with: a) high spatial and temporal variability of the chlorophyll-*a* concentration and primary production; b) a low vertical resolution of the observed profiles of these characteristics (only 3—5 measurements); c) errors due to the fixation of the Chla:C ratio in phytoplankton.

Cost function for modeled and observed primary production (PP) and chlorophyll-*a* concentration (Chla). Dash stands for the absence of observations

Функция качества для модельных и измеренных данных по первичной продукции (PP) и концентрации хлорофилла-*a* (Chla)

	Sval_2	Bar_5	Pech_8	Kara_1	KaraE_1
PP	0.36	–	–	0.16	0.59
Chla	0.63	0.85	0.65	1.23	1.05

Прочерк означает отсутствие данных наблюдений

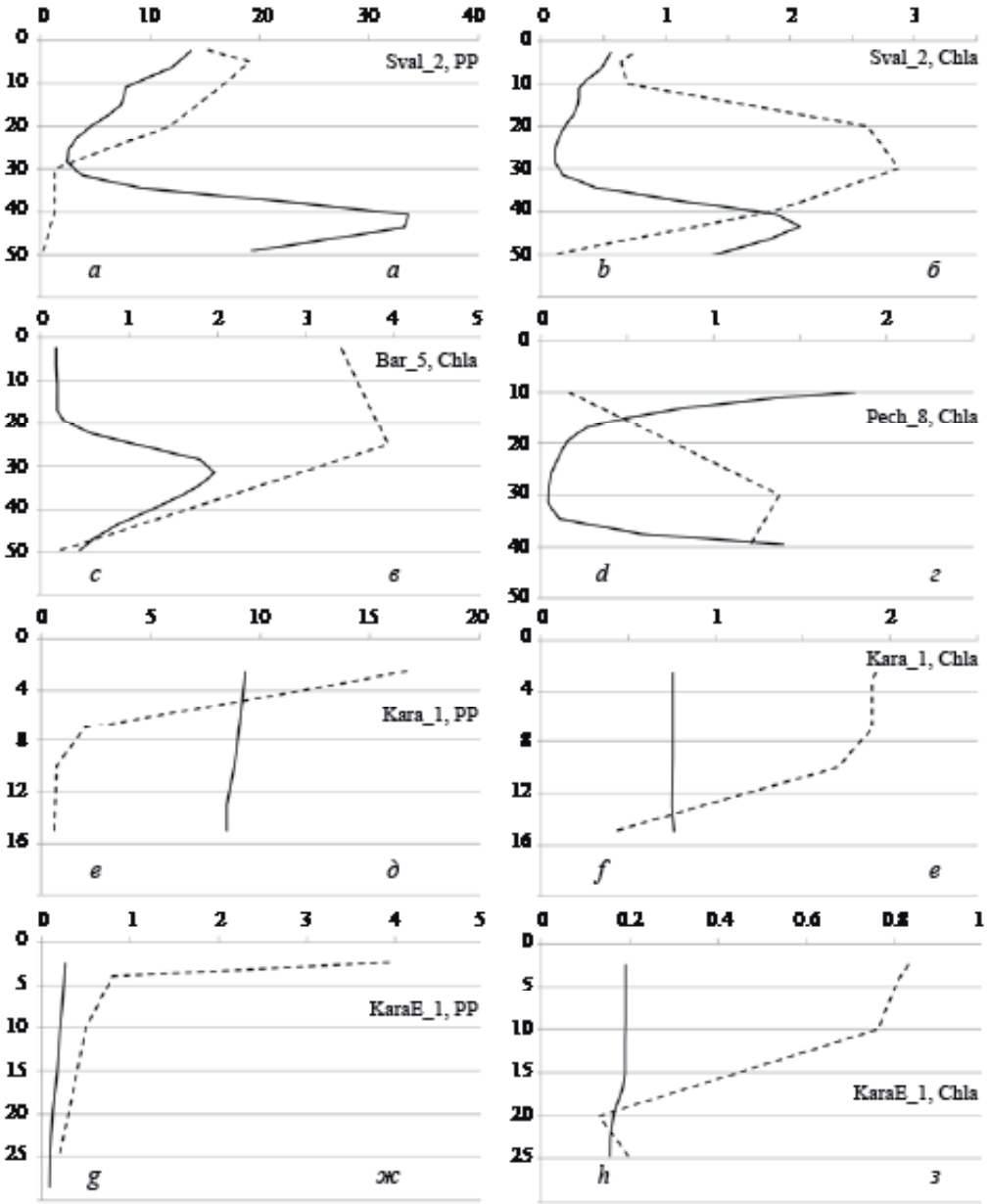

Fig. 3. Vertical profiles of chlorophyll-a concentration Chla [mg/m3] and primary production PP [mg C/m^3/day] for different locations and dates: *a* — Sval_2, PP, 05.07.2001; *b* —Sval_2, Chla, 05.07.2001; *c* —Bar_5, Chla, 16.06.1993; *d* — Pech_8, Chla, 15.07.1993; *e* —Kara_1, PP, 02.09.1993; *f* —Kara_1, Chla, 02.09.1993; *g* — KaraE_1, PP, 24.09.1993; *h* —KaraE_1, Chla, 24.09.1993. Solid line — model, dashed line — observations.

Рис. 3. Вертикальные профили концентрации хлорофилла-а Chla [мг/м3] и первичной продукции PP [мг С/м^3/день] для различных точек и дат: *а* — Sval_2, PP, 05.07.2001; *б* — Sval_2, Chla, 05.07.2001; *в* — Bar_5, Chla, 16.06.1993; *г* — Pech_8, Chla, 15.07.1993; *д* — Kara_1, PP, 02.09.1993; *е* — Kara_1, Chla, 02.09.1993; *ж* — KaraE_1, PP, 24.09.1993; *з* —KaraE_1, Chla, 24.09.1993. Сплошная линия — модель, пунктирная — наблюдения.

3. Results

Distribution of chlorophyll-a surface concentration. An analysis of the intra-annual variability of the calculated chlorophyll-*a* surface concentration and the position of the marginal ice zone has been made, with the year 2003 taken as an example (Fig. 4, see an insert). As follows from the results, in 2003 the beginning of the intensive phytoplankton bloom in the Barents Sea occurred at the beginning of May (Fig. 4, *a*). At this time a zone of increased chlorophyll-*a* concentration (1.5—2.5 mg/m^3) was clearly distinguishable and bordering with

the position of pack ice edge represented by the isoline of ice compactness Ci=0.8. It should be noted that the bloom occurred in so-called marginal ice zone (0.15<Ci<0.8), the chlorophyll-*a* concentrations under the ice in the presented results being equal about 0.5—1.0 mg/m^3 and sometimes even higher. This is an important feature of the marine ecosystem functioning in the Arctic region [34—36]. According to [36], a spring phytoplankton bloom begins when the short-wave solar radiation (SWR) at the sea surface reaches the values of about 100 W/m^2, and PAR is about 40 W/m^2. This level of SWR, required for the onset of the bloom, is determined both by the thickness of snow on the ice surface and by the ice compactness Ci and is achieved with complete disappearance of snow and when Ci≈0.5. These conditions for the spring phytoplankton bloom are typical for the entire Barents Sea: the start of bloom is always due to the reaching of the required level of SWR (not less than 100 W/m^2) in open water or in the marginal ice zone in the absence of snow on its surface [36].

According to the results obtained, the peak of the phytoplankton bloom in the Barents Sea occurred at the end of May — the beginning of June (Fig. 4, *b* and *c*), with chlorophyll-*a* concentrations reaching 13—15 mg/m^3 in the central regions of the sea. The retreat of the ice cover to the northeast led to the splash of phytoplankton growth along the northwestern coast of the Novaya Zemlya archipelago where the same pattern was observed: the maximum concentrations were observed along the retreating ice edge. After that, the maxima of chlorophyll-*a* surface concentrations in the Barents Sea shifted northward while in the central regions of the Barents Sea the concentrations became relatively small (0.5—2.0 mg/m^3).

The start of the intense phytoplankton bloom in the Kara Sea in 2003 (Fig. 4, *d* and *e*) occurred on June 20—25 when the sea gradually began to be released from the ice. Let us note one more interesting detail of the obtained results: at the beginning of the bloom period in the Kara Sea the maximum surface concentrations of chlorophyll-*a* (6—7 mg/m^3) were observed almost under the ice cover (Fig. 4, *d*), in the area between Novaya Zemlya archipelago and the Yamal Peninsula. Later these increased concentrations were already observed in the regions less covered with ice (Fig. 4, *e*).

Mid-late July (Fig. 4, *f*) and also August and September 2003 were characterized by significantly lower surface chlorophyll-*a* concentrations, with an average surface concentration of about 0—2 mg/m^3 and without pronounced local maxima.

The results obtained for the spatial distribution of the surface concentration of chlorophyll-*a*, in general, were in agreement with the satellite measurements presented in the open access at the website https://oceancolor.gsfc.nasa.gov for the above-mentioned period.

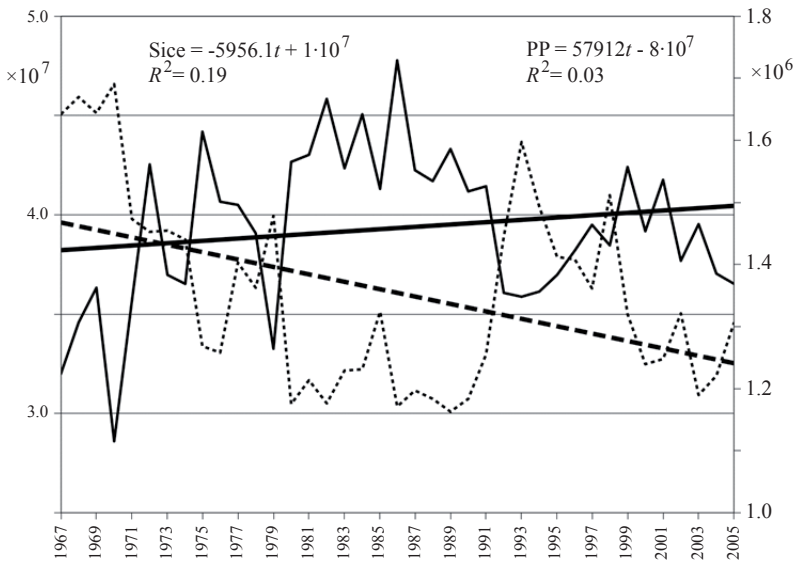

Fig. 5. Interannual variability of the integrated over the entire domain primary production (solid line, [mmol N/s], left scale) and the total area of sea ice (dashed line, [km^2], right scale), both time-averaged over the hydrological year (from October to September). Year order: 1967 means October 1966—September 1967.

Рис. 5. Межгодовая изменчивость средних за гидрологический год (с октября по сентябрь) интегральной первичной продукции (сплошная линия, [ммоль N/с], левая шкала) и суммарной площади льда (пунктирная линия, [км^2], правая шкала) в модельной области. Нумерация лет: 1967 г. означает октябрь 1966—сентябрь 1967.

Relationship between primary production and sea ice area. A more general view of the nature of fluctuations in primary production in the study area can achieved by the analysis of the behavior of integrated over the entire domain primary production which, alongside with the total area of sea ice, is shown in Fig. 5. Both two characteristics have been time-averaged over the hydrological year (from October to September). As can be seen, during the period under study (1966—2005) the trend is negative for the total sea ice area (trend is significant, p-level = 0.006), i.e. the total area of sea ice in the Barents, Kara and White Seas has been decreasing during the second part of the 20th century due to the observed climate warming in this period. The trend is insignificant (p-level = 0.30) for primary production.

It is well-known that the trend's estimate strongly depends on the length of the time series. If we consider the period of 1966—1992 then it is obvious that both characteristics changed in antiphase and their trends were significant and opposite, so that with a rapid decrease in the sea ice total area the phytoplankton primary production increased significantly. However, since 1993, despite the persisting opposition of the two characteristics, their trend magnitude had been decreasing, which led to its disappearance for primary production. In 1999—2000 there occurred a 'failure' of this relationship and primary production began to decline along with the continuing declining of the total sea ice area. Perhaps other limiting factors began to prevail, e.g. reduced PAR due to the possible increase of cloudiness in the Arctic Ocean. This hypothesis has yet to be verified.

Correlation coefficient between annual values of integral primary production and the total sea ice area (both averaged over the hydrological year) for the period 1966—2005 is −0.80. The same coefficient but calculated between primary production and the sea ice area with ice compactness Ci>0.15 is equal to −0.80 as well, and between primary production and the pack ice area (Ci>0.8) is equal to −0.82. Since the averaging for a hydrological year mainly characterizes the ice area in winter and primary production in spring when these characteristics are maximal, then the small ice cover area in the previous winter can be considered as one of the main reasons for the increase in primary production in the current year. We would like to note that in the paper [35] where the relationship between the average annual primary production and the total sea ice area for the whole Arctic Ocean was estimated for 1998—2007, the correlation coefficient was -0.89. However, in the present work for the same period of 1998—2007 for the region under consideration (the White, Barents and Kara Seas) such correlation did not hold (see Fig. 5).

In addition, the analysis of the fluctuations in the area of pack ice (ice compactness Ci>0.8) and the summed area of pack ice and marginal ice zone (Ci>0.15) has shown that the area of pack ice decreased slower. In other words, less compact ice melted faster. This is naturally explained by the increase of the contact surface area between water and ice in the process of ice compactness reduction.

As was shown above, during the algae bloom a significant part of primary production was located in the marginal ice zone with sea ice compactness 0.15<Ci<0.8. Fig. 6 shows the intra-annual primary production (PP) integrated over the whole model domain, marginal ice zone area (Smiz), and the total sea ice area (Sice) in certain years of the period under study. The annual curve of Smiz is characterized by two maxima during a year — a large in spring and a small in autumn. The spring maximum is formed during the melting and destruction of the ice cover. This process is accompanied by the detachment of individual ice floes from the pack ice with their subsequent drift in ice-free areas. As a result, the Smiz area first increases, reaching a maximum in late June — early July, and then decreases to a minimum in August-September as the one-year ice melts. A small autumn maximum of Smiz is associated with a rapid increase of the area of thin ice at the beginning of its formation in late autumn. During this process the area of pack ice remains practically unchanged while the subsequent reduction in the area of thin ice occurs as the thickness and compactness of ice increase. Figs. 6, *a* and *c* show that during any year the peak of primary production integrated over the entire domain occurs almost synchronously with the maximum of the marginal ice zone area (Smiz). During the vegetation period, which coincides with the period of the light day in the Arctic (from March to October), the synchronous correlation coefficient between the Smiz and the integral primary production is equal to 0.87. At the same time, figs. 6, *b* and *d* show that the total sea ice area behaves absolutely differently: a sharp decrease in the total ice area is observed in spring and leads to the intensive growth of primary production. But in this case the correlation coefficient between the daily values of the total sea ice area and the integral primary production is only −0.36.

4. Discussion and Conclusions. The estimates of the spatial distribution of the chlorophyll-*a* concentration in the surface layer have clarified the effect of sea ice on primary production in the Arctic seas, including under conditions of a changing climate that leads to a significant reduction of ice cover in the Arctic Ocean.

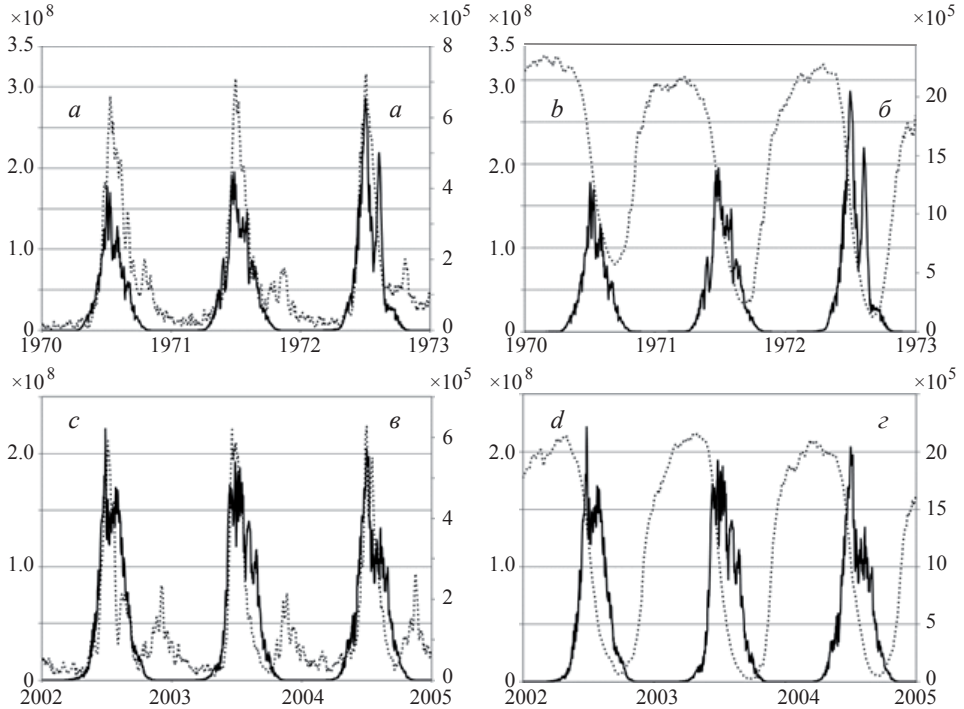

Fig. 6. Intra-annual variability of the integrated over the entire domain primary production PP (solid line, [mmol N/s], left scale), marginal ice zone area (Smiz) and the total area of sea ice (Sice) (both are shown by dotted line, [km^2], right scale) in the beginning and in the end of the study period. *a* — PP and Smiz, 1970—1972; *b* — PP and Sice, 1970—1972; *c* — PP and Smiz, 2002—2004; *d* —PP and Sice, 2002—2004.

Рис. 6. Внутригодовой ход интегральной по модельной области первичной продукции PP (сплошная линия, [ммоль N/с], левая шкала), площади маргинальной зоны льда (Smiz) и общей площади льда (Sice) (обе обозначены пунктирной линией, [км^2], правая шкала) в начале и в конце рассматриваемого периода. *а* — PP и Smiz, 1970—1972; *б* — PP и Sice, 1970—1972; *в* — PP и Smiz, 2002—2004; *г* — PP и Sice, 2002—2004.

The clear relationship between the area of the marginal ice zone and primary production has been obtained: the moments of their spring-summer peaks coincide completely and they are highly correlated (0.87), proving the importance of this zone in the functioning of the marine ecosystem. As expected, the interannual variability of the integrated primary production and the total sea ice area (both averaged over the hydrological year — from October to September) have demonstrated an antiphase oscillation which means that the reduced sea ice cover area in previous winter is one of the main reasons for the increase in primary production in a current year.

The drawbacks of the obtained solution are primarily due to the simplicity of the biogeochemical model being used. It is well-known that in the Arctic regions diatoms constitute a significant part of phytoplankton biomass. Diatoms are limited not only by PAR and inorganic nitrogen but also by inorganic silicon. Also in reality there is a change in the prevailing species of phytoplankton during the vegetation period. These aspects of the functioning of the marine ecosystem lower trophic level are not described by the current biogeochemical model, in which there is only a 'generalized' phytoplankton limited only by the concentration of nitrates and shortwave radiation. In addition, the adoption of a constant chlorophyll-to-carbon ratio in phytoplankton is a rather crude assumption. We should also note that for the correct description of the remineralization process in such shelf regions as the Barents and Kara Seas it is desirable to use some benthic model that is currently absent in the model ecosystem block.

The results of section 2.1 were obtained in the framework of the state assignment of FASO Russia (theme No. 0149-2018-0014). The results of section 2.2 were obtained within the Program of Fundamental Research of the RAS Presidium I.49 (theme of the state assignment No. 0149-2018-0027). The results of section 3 were obtained within the grant of the Russian Foundation for Basic Research (RFBR) (project No. 16-55-76021). The work was supported by the ERA-Net project EXOSYSTEM (grant agreement 01DJ16016) funded by the Federal Ministry for Education and Research (Germany). The simulations were performed at the German Climate Computing Center (DKRZ).

Литература

1. *Pabi S., van Dijken G. L., Arrigo K. R.* Primary production in the Arctic Ocean, 1998—2006 // J. Geophys. Res. 2008. 113. C08005. doi:10.1029/2007JC004578.
2. Research Fronts 2014: The National Science Library, Chinese Academy of Sciences, Thomson Reuters IP & Science, The Joint Research Center of Emerging Technology Analysis, 2014, 62 p.
3. Research Fronts 2016. Institutes of Science and Development, Chinese Academy of Sciences, The National Science Library, Chinese Academy of Sciences, Clarivate Analytics, 2016, 104 p.
4. Research Fronts 2017. Institutes of Science and Development, Chinese Academy of Sciences, The National Science Library, Chinese Academy of Sciences, Clarivate Analytics, 2017, 94 p.
5. *Fasham M. J. R., Ducklow H. W., McKelvie S. M.* A nitrogen-based model of plankton dynamics in the oceanic mixed layer // Journal of Marine Research. 1990. 48. 591—639.
6. *Popova E. E., Yool A., Aksenov Y., Coward A. C., Anderson T. R.* Regional variability of acidification in the Arctic: a sea of contrasts // Biogeosciences. 2014. 11. 293—308. doi:10.5194/bg-11-293-2014
7. *Yool A., Popova E. E., Anderson T. R.* Medusa-1.0: a new intermediate complexity plankton ecosystem model for the global domain // Geosci. Model Dev. 2011. 4. 381—417. doi:10.5194/gmd-4-381-2011
8. *Yool A., Popova E. E., Anderson T. R.* MEDUSA-2.0: an intermediate complexity biogeochemical model of the marine carbon cycle for climate change and ocean acidification studies // Geosci. Model Dev. 2013. 6. 1767—1811. doi:10.5194/gmd-6-1767-2013
9. *Popova E. E., Yool A., Coward A. C., Aksenov Y. K., Alderson S. G., de Cuevas B. A., Anderson T. R.* Control of primary production in the Arctic by nutrients and light: Insights from a high-resolution ocean general circulation model // Biogeosci. 2010. 7(11). 3569—3591. doi:10.5194/bg-7-3569-2010.
10. *Popova E. E., Yool A., Aksenov Y., Coward A. C.* Role of advection in Arctic Ocean lower trophic dynamics: a modeling perspective // J. Geophys. Res. Oceans. 2013. 118. doi:10.1002/jgrc.20126
11. *Zhang J., Spitz Y. H., Steele M., Ashjian C., Campbell R., Berline L., Matrai P.* Modeling the impact of declining sea ice on the Arctic marine planktonic ecosystem // J. Geophys. Res. 2010. 115. C10015. doi:10.1029/2009JC005387.
12. *Kishi M. J. M.* et al. NEMURO — A lower trophic level model for the North Pacific marine ecosystem // Ecol. Model. 2007. 202. 12—25.
13. *Meibing Jin, Clara Deal, Sang H. Lee, Scott Elliott, Elizabeth Hunke, Mathew Maltrud, Nicole Jeffery.* Investigation of Arctic sea ice and ocean primary production for the period 1992—2007 using a 3-D global ice–ocean ecosystem model // Deep-Sea Research II 2012. 81—84, 28—35.
14. *Moore J. K., Doney S. C., Kleypas J. C., Glover D. M., Fung I. Y.* An intermediate complexity marine ecosystem model for the global domain // Deep-Sea Res. 2002. II 49. 403—462.
15. *Moore J. K., Doney S. C., Lindsay K.* Upper ocean ecosystem dynamics and iron cycling in a global three-dimensional model // Global Biogeochem. Cycles 18. 2004. GB4028. doi:10.1029/2004GB002220.
16. *Lebedeva L. P., Shushkina E. A., Vinogradov M. E.* A dynamic model of the pelagic ecosystem of the Kara Sea // Oceanology. 1995. 34 (5). 661—666.
17. *Аверкиев А. С.* Моделирование формирования зоны высокой первичной продуктивности над поднятием дна в Баренцевом море при прохождении циклона // Вестник Северного (Арктического) Федерального Университета, Сер. Естественные науки. 2014. №3. С. 5—14.
18. *Filatov N., Pozdnyakov D., Johannessen O. M., Pettersson L. H., Bobylev L. P.* White Sea: Its marine Environment and ecosystem dynamics influenced by global change. Chichester: Springer-Praxis Publ., 2007. 476 p.
19. *Толстиков А. В., Чернов И. А., Мурзина С. А., Мартынова Д. М., Яковлев Н. Г.* Разработка комплекса GREEN JASMINE для изучения и прогнозирования состояния экосистем Белого моря // Труды Карельского научного центра РАН. 2017. № 5. С. 23—32.
20. *Vichi M., Pinardi N., Masina S.* A generalized model of pelagic biogeochemistry for the global ocean ecosystem. Part I: theory // Journal of Marine Systems. 2007a. 64. C. 89—109.
21. *Vichi M., Masina S., Navarra A.* A generalized model of pelagic biogeochemistry for the global ocean ecosystem. Part II: numerical simulations // Journal of Marine Systems, 2007b. 64. P. 110—134.
22. *Sein D. V., Mikolajewicz U., Groger M., Fast I., Cabos W., Pinto J. G., Hagemann S., Semmler T., Izquierdo A., Jacob D.* Regionally coupled atmosphere-ocean-sea ice-marine biogeochemistry model ROM: 1. Description and validation // J. Adv. Model. Earth Syst. 2015. 7. P. 268—304.
23. *Marshall J., Adcroft A., Hill C., Perelman L., Heisey C.* A finite-volume, incompressible navier-stokes model for studies of the ocean on parallel computers // J. Geophys. Res. 1997. 102(C3). 5753—5766. 1997.
24. *Danilov S.* Ocean modeling on unstructured meshes // Ocean Modelling. 69. 195—210. 2013. DOI: 10.1016/j.ocemod.2013.05.005
25. *Hibler III W. D.* A dynamic thermodynamic sea ice model // J. Phys. Oceanogr. 9. 815—846. 1979.
26. *Hibler III W. D.* Modeling a variable thickness sea ice cover // Mon. Wea. Rev. 1. 1943—1973. 1980.
27. *Zhang J., Hibler III W. D.* On an efficient numerical method for modeling sea ice dynamics // J. Geophys. Res. 102(C4). 8691—8702. 1997.
28. *Losch M., Menemenlis D., Campin J.-M., Heimbach P., Hill C.* On the formulation of sea-ice models. Part 1: Effects of different solver implementations and parameterizations // Ocean Modelling. 2010. 33(1–2), 129—144. doi:10.1016/j.ocemod.2009.12.008
29. *Martyanov S. D., Dvornikov A. Yu., Gorchakov V. A., Losa S. N.* Model estimates of the ecosystem contribution in the carbon dioxide exchange between the ocean and the atmosphere in the Barents Sea // Фундаментальная и прикладная гидрофизика. 2017. Т. 10, № 1. С. 11—16.

30. *Zhang J. L., Rothrock D. A.* Modeling global sea ice with a thickness and enthalpy distribution model in generalized curvilinear coordinates // Mon. Weather Rev. 2003. 131. P. 845—861.
31. *Schweiger A., Lindsay R., Zhang J., Steele M., Stern H.* Uncertainty in modeled arctic sea ice volume // J. Geophys. Res. 2011. 116, C00D06. doi:10.1029/2011JC007084.
32. *Matrai P.* and Bigelow Laboratory for Ocean Sciences (2011). Productivity, chlorophyll a, Photosynthetically Active Radiation (PAR) and other phytoplankton data from the Arctic Ocean, Bering Sea, Chukchi Sea, Beaufort Sea, East Siberian Sea, Kara Sea, Barents Sea, and Arctic Archipelago measured between 17 April, 1954 and 30 May, 2006 compiled as part of the Arctic System Science Primary Production (ARCSS-PP) observational synthesis project (NODC Accession 0063065). Version 1.1. National Oceanographic Data Center, NOAA. Dataset. (Дата обращения: 01.07.2015).
33. *Radach G., Moll A.* Review of three-dimensional ecological modelling related to the North Sea shelf system. Part II: model validation and data needs // Oceanography and Marine Biology: An Annual Review, 2006, 44, P. 1—60.
34. *Kushnir V., Pavlov V., Morozov A., Pavlova O.* “Flashes” of chlorophyll-a concentration derived from in Situ and remote sensing data at the Polar Front in the Barents sea // The Open Oceanography Journal. 2011. 5, P. 14—21.
35. *Jin M., Deal C., Lee S. H., Elliott S., Hunke E., Maltrud M., Jeffery N.* Investigation of Arctic sea ice and ocean primary production for the period 1992—2007 using a 3-D global ice–ocean ecosystem model // Deep-Sea Res. 2012. II. 81—84, 28—35.
36. *Рябченко В. А., Горчаков В. А., Дворников А. Ю., Пугалова С. С.* Оценки влияния ледового покрова на первичную продукцию фитопланктона в Баренцевом море (по результатам трехмерного моделирования) // Фундаментальная и прикладная гидрофизика. 2016. Т. 9, № 1. С. 41—51.

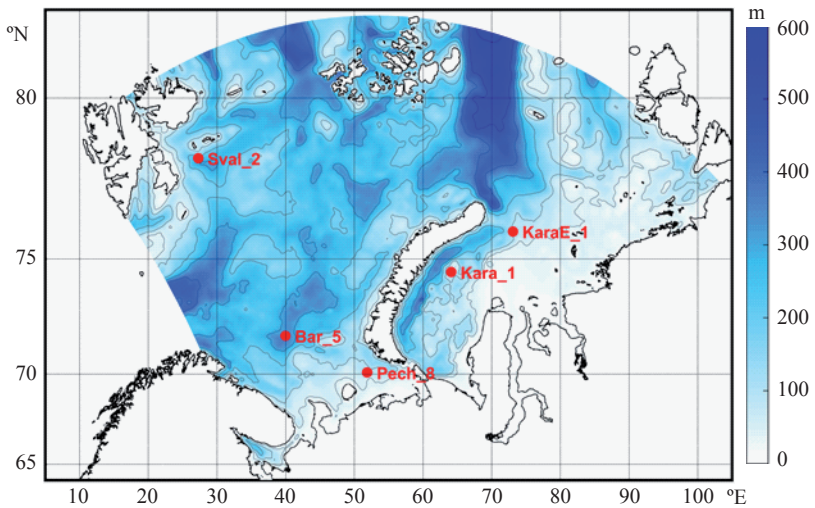

Fig. 1. Model domain and bathymetry. Points mark the locations of five observation stations: (Sval_2: 78.358 N, 27.265 E, 2001), (Bar_5: 71.82 N, 39.97 E, 1993), (Pech_8: 70.08 N, 51.87 E, 1993), (Kara_1: 74.50 N, 64.10 E, 1993), (KaraE_1: 76.00 N, 73.10 E, 1993).

Рис. 1. Модельная область и карта глубин. Точками отмечены пять станций наблюдений: (Sval_2: 78,358 N, 27,265 E, 2001), (Bar_5: 71.82 N, 39.97 E, 1993), (Pech_8: 70.08 N, 51.87 E, 1993), (Kara_1: 74.50 N, 64.10 E, 1993), (KaraE_1: 76.00 N, 73.10 E, 1993).

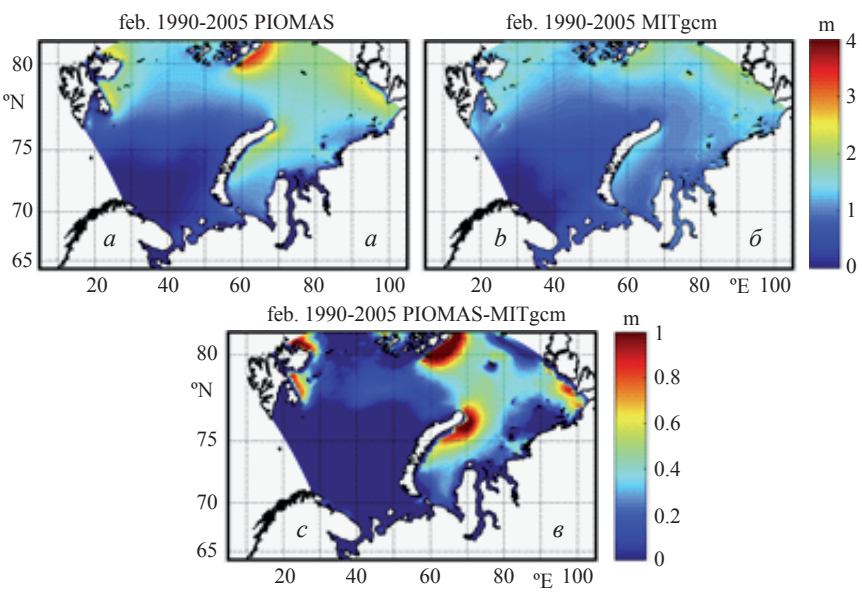

Fig. 2. Monthly-mean sea ice thickness in February averaged over the period 1990—2005.
a — PIOMAS data; *b* — Model results; *c* — Difference (PIOMAS-Model).

Рис. 2. Среднемесячная толщина льда в феврале, осредненная за период 1990—2005 г.
а — данные архива PIOMAS; *б* — результаты модели; *в* — разность (PIOMAS-Модель).

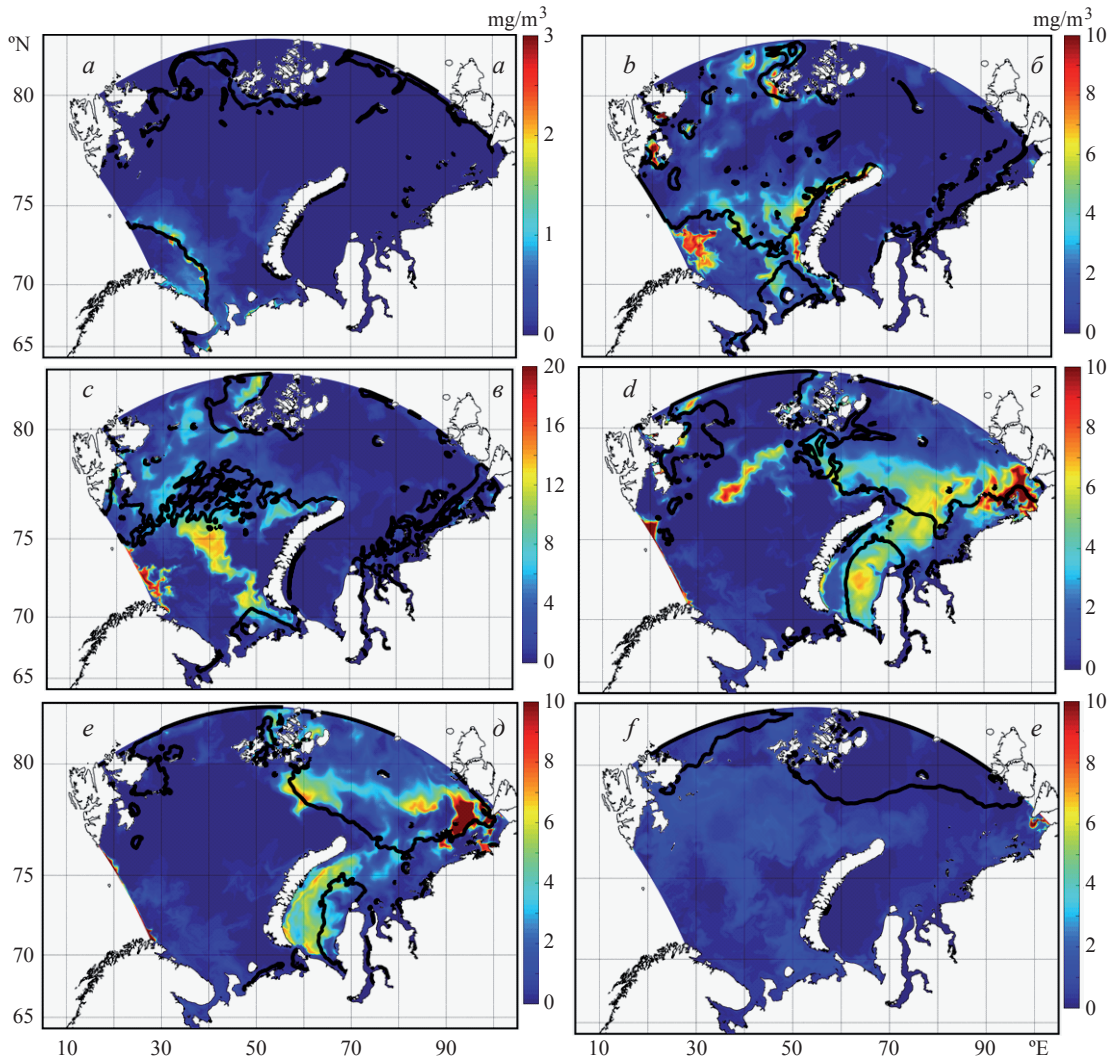

Fig. 4. Modeled chlorophyll-*a* surface concentration and the position of 0.8-isoline of the sea ice compactness (ice edge): *a* — 01.05.2003; *b* — 31.05.2003; *c* — 07.06.2003; *d* — 20.06.2003; *e* — 25.06.2003; *f* — 18.07.2003.

Рис. 4. Рассчитанная поверхностная концентрация хлорофилла-*a* и положение изолинии сплоченности льда 0.8 (кромка льда): *а* — 01.05.2003; *б* — 31.05.2003; *в* — 07.06.2003; *г* — 20.06.2003; *д* — 25.06.2003; *е* — 18.07.2003.